RESCUE: PASSIVE WIRELESS SENSOR NETWORK ARCHITECTURE FOR EARTHQUAKE RESCUE APPLICATION

by

Orkhan Badirkhanli

A Thesis Submitted to the
Graduate School of Engineering
in Partial Fulfillment of the Requirements for
the Degree of

Master of Science

in

Electrical and Electronics Engineering

Koç University

AUGUST 2014

Koç University

Graduate School of Sciences and Engineering

This is to certify that I have examined this copy of a master's thesis by

Orkhan Badirkhanli

and have found that it is complete and satisfactory in all respects,

and that any and all revisions required by the final

examining committee have been made.

Committee Members:

Özgür B. Akan, Ph. D. (Advisor)

Sinem Çöleri Ergen, Ph. D.

Öznur Özkasap, Ph. D

Date: ______________________________

Anneme ve Babama,

Kamila Guliyeva ve Ilham Badirkhanov.

ABSTRACT

In a disaster situation such as an earthquake it is vital to know the number of people left under ruins. To address this problem, we propose RESCUE - wiREless backScattering CommUnication-based disastEr recovery system. To the best of our knowledge, this is the first solution based on passive communication to be applied for disaster recovery to reveal people count inside collapsed building. RESCUE is composed of special RFID reader and sensors that are used to determine the total number of people under ruins. Passive wireless sensor nodes are placed inside building during construction and are equipped with a camera that is activated in case of an earthquake and takes pictures of building interior. After an earthquake, backscattering communication is used by the reader located outside ruins to read image data from sensors. The images are used to evaluate the number of people present inside building just before the earthquake. We analyse passive communication channel between RESCUE reader and sensors. We derive passive wireless communication channel model over ruins and carry out simulations using a modified passive RFID simulator. Furthermore, we obtain the results of experimental study where we validate the derived channel model. Results show that RESCUE can provide high performance of data collection in relatively short time period, and hence, is a promising disaster recovery system architecture.

ÖZETÇE

Deprem gibi bir afet zamanında, enkaz altında kalmış insan sayısını bilmek hayati onem taşır. Bu problemi ele almak icin bu çalışmada RESCUE - Kablosuz Geri Saçılım Temelli Afet Yönetimi Sistemi önerilmektedir. Bilgimiz çerçevesinde, bu sistem, çökmüş binaların altında kalmış insan sayısını belirlemek için afet yönetimi sürecine uygulanmış olan ilk cozümdür. RESCUE, yıkıntı altında kalmış toplam insan sayısını belirlemek için ozel tasarlanmış RFID okuyucu ve sensörlerden oluşmaktadır. Deprem anında binanın içerisinin resimlerini çeken bir kameraya sahip olan pasif kablosuz sensör düğümleri bina yapım zamanı binanın içine kurulur. Deprem sonrasında, yıkıntının dışarısında bulunan okuyucu geri saçılımlı haberleşme aracılığı ile sensörlerin içindeki görüntü bilgisini okur. Bu resimler, depremin hemen öncesinde binanın içinde bulunan insan sayısını hesaplamak için kullanılır. Bu çalısmada RESCUE okuyucu ve sensörleri arasındaki pasif haberleşme kanalının analizi yapılmaktadır. Bunun için pasif kablosuz haberleşme kanalı modellenmekte ve pasif RFID simülatörü kullanılarak simülasyonlar gerçekleştirilmektedir. Ayrıca, çıkarılmış kanal modelini doğrulamak icin yapılan deneysel calışmanın sonuçları sunulmaktadır. Deney sonuçları, RESCUE'nun nispeten kısa sürede yüksek performansla veri toplanmasını sağladığını ve bu nedenle, umut vadeden bir afet yönetimi sistemi olduğunu göstermektedir.

ACKNOWLEDGMENTS

Firstly, I want to express my sincere gratitude to my supervisor, Dr. Özgür Barış Akan for his encouragement, valuable advices and worthy counselling. I appreciate his consistent guidance and help in all stages of my study.

I want to thank members of my thesis jury, Dr. Sinem Çöleri Ergen and Dr. Öznur Özkasap for their critique and effort.

A note of thanks to the Ankaref Information Technologies company that provided key equipment required for the realization of the experimental study for this thesis.

I would like to thank members of Next-generation Wireless Communication Laboratory (NWCL) for their warm company, with whom I shared valuable moments.

Finally, I am deeply grateful to all my family members for their inspiration, confidence in me and love. I express my candid acknowledgement to them for their support all though my master study.

TABLE OF CONTENTS

LIST OF TABLES

LIST OF FIGURES

ABBREVIATIONS

RESCUE	wiREless backScactering CommUnication based disastEr recovery system
RFID	Radio Frequency Identification
EPC C1Gen2 RFID	EPC Class 1 Generation 2 Radio Frequency Identification
ACK	Acknowledgement
UHF	Ultra High Frequency
BER	Bit Error Rate
SNR	Signal to Noise Ratio
AWGN	Additive White Gaussian Noise
LOS	Line Of Sight
EIRP	Equivalent Isotropically Radiated Power
USRP	Universal Software Radio Peripheral
CW	Continuous Wave
PIE	Pulse Interval Encoding
ASK	Amplitude Shift Keying
MAC	Media Access Control

Chapter 1

INTRODUCTION

During search and disaster recovery operations after an earthquake, disaster recovery teams are interested in rescuing maximum number of people under building ruins in the shortest time. This is critical because death toll after a building collapse dramatically increases with time [1,2]. Generally, search and rescue of trapped people under rubble involves several phases. In the initial phases of operation, rescue workers conduct a structural assessment where they try to identify basic characteristic of the disaster scenario such as the structure involved, the number of victims buried and their locations [3]. Current techniques used for this phase involve the use of sound detecting devices, victim location identification with the use of trained dogs, visual spot examination [4] and witness questioning [3]. However, these techniques come short in extracting conclusive and accurate information about trapped victims. Therefore, reliable and robust systems need to be employed to rescue as many alive people as possible.

1.1 Research Objectives and Solutions

Research objectives, the system that we propose and other solutions are described in this section.

1.1.1 Disaster Rescue Process

Two main problems that need to be addressed during victim rescue operation are identifying total number of people trapped inside a rubble and predicting their possible locations. Once this information is available, rescue teams and the first responder can be allocated more efficiently to remove victims under building ruins in the shortest possible time. Using a system to track already rescued people, rescue teams can obtain data about how many more people are left inside collapsed building.

Presently, no technology exists that can provide data on victim count after an earthquake. Researchers have proposed various ways to achieve this using passive RFID tags [5, 6]. However, performance evaluation of these proposed approaches is missing. Studies have been carried out in the quest for improving currently available methods using both passive RFID tags and other means such as snake like robots, radar systems, mobile phone localization [6–10]. However, these studies are incomplete to be used for victim detection, as they sometimes lack an important aspect of a problem being solved such as appropriate communication channel model formulation, signal interference resolution and performance analysis.

1.1.2 RESCUE - Wireless Backscattering Communication Based Disaster Recovery System

In this study, we present RESCUE, which, to the best of our knowledge, is the first wireless backscattering communication-based disaster recovery system that is able to provide vital information, e.g., the number of people trapped under ruins and their probable locations, which can be used during search and rescue operations. RESCUE consists of a special UHF RFID reader and passive sensors [11], equipped with passive UHF RFID tags. RESCUE sensors are installed inside a building during (or after) construction and the reader is used during disaster recovery process by the rescue teams. Sensors store up-to-date image information of building interior such as corridors and apartment rooms. After an earthquake, RESCUE reader is used to collect image data from sensors under ruins for the purpose of calculating the total number of people and their last location information before an earthquake. After data is collected, an automatic human detection algorithm or manual operators are employed to analyze images to count the number of people present in every image and note their location just before earthquake. The details of identifying people using any of the existing image recognition techniques is beyond the scope of this study. The location and ID of every sensor is assumed to be known, so that an agent can readily identify the locations in images.

1.1.3 Power Loss and RESCUE Reader Transmission Power

To make decisions on characteristics of both sensors and reader, we have studied passive communication between them in a channel with rubble. As communication through rubble contains many obstacles, mainly made of concrete, brick and other construction materials, the signal strength attenuation through these materials need to be considered when formulating a model. In addition, because of the clutter in the channel, wireless communication will contain many multipath components. Number of studies exist that study power loss through building ruins [12–14]. However, these studies either ignore some of the factors that contribute to the total power loss or present a channel model that cannot fully characterize the communication through densely cluttered building ruins. We develop a model, where we take into account path loss, multipath fading and shadowing that occur during communication through rubble.

To describe power loss over building ruins, we use an earthquake simulator software [15]. After constructing a building, earthquakes with various parameters can be applied to the building with the simulator to obtain different collapse structures. By means of these collapses, we evaluate power loss between reader outside the ruins and the sensors at different locations inside the ruins. This information is important as it is the main parameter considered for determining the required transmission power for the reader.

When communicating with a passive RFID tag, a reader needs to transmit sufficient power so that the tag circuit activates and backscatters the data stored on it. This is especially challenging over a channel within ruins. We calculate the required transmission power needed for the RESCUE reader to collect data from passive sensors located under debris of different size buildings.

1.2 Performance of RESCUE

The theoretical study of passive wireless communication between RESCUE reader and sensors is performed using an UHF RFID simulator. By adding new features to the existing RFIDSim [16] open source simulator, we were able to perform thorough analysis of RESCUE. Since the channel bit-error-rate (BER) can deteriorate communication throughput between the reader and sensors, the amount of data that a sensor sends to the reader in each request needs to be appropriately determined. Thus, depending on channel BER, the optimal amount of data to be sent for each request has been calculated and used in the simulations. Optimizing requested data amount served to minimize total read time of sensors, and, in turn, contributed to minimization of total electromagnetic energy radiation.

1.3 Experimental Study

To validate the possibility of reading a passive sensor under ruins, we have also carried out an experimental study. We placed a standard UHF RFID reader and an RFID tag in an environment, where they are separated by a medium made of reinforced concrete, brick and other construction materials. By using a directional antenna on reader, we were able to read data on a tag. Using spectrum analyser, we have measured received power level near the tag to experimentally calculate the channel power loss. Our measurements confirmed the results predicted by theoretical channel model.

1.4 Thesis Outline

The rest of the thesis is organized as follows. In Chapter 2, we present the related work. In Chapter 3, RESCUE system architecture is given, where we discuss the details of our proposed approach. The channel model is introduced in Chapter 4, where power loss model and transmission power are given. Chapter 5 presents the performance analysis, where the results of simulations are presented. In Chapter 6, we discuss the details of experimental study and compare the results. Finally, conclusion is given in Chapter 7.

Chapter 2

RELATED WORK

In this chapter, we examine related studies. We state the contributions and shortcomings of current research on this topic.

2.1 The Use of RFID Technology During Disaster Recovery

The use of RFID tags during disaster relief situations have been proposed in a number of studies. Resource management during rescue operations and possible advantages of using RFID tags have been discussed in [17], [18]. Several other studies have proposed using RFID tags for handling disaster victims, allocation of rescue teams and their coordination. In [19], authors discuss attaching RFID tags to people rescued from ruins for ease of tracking their medical condition. The same also study proposes adhering RFID tags in various places inside disaster site and using them as a message board by rescue teams for sharing information on existence of victims in specific places. Similar applications have also been examined in [6] and [20]. Placing RFID tags on collapsed building and forming an Ad-Hoc network of mobile devices such as mobile phones, PDAs and tablet PCs with RFID readers for distribution of structural integrity information among structural engineering and rescue workers is presented in [21]. Even though these studies suggest different techniques that RFID technology can be used to mitigate the effects of a disaster scenario such as an earthquake, they do not analyze the performance of the proposed techniques.

2.2 The Use of RFID Technology for Finding Disaster Victims

The idea of utilizing RFID tags for directly finding victims trapped under ruins have also been proposed in [6]. A reader outside the rubble would read the tags attached to victims and report their location. However, to address the task of locating a tag under building ruins with a reader outside the ruins, the communication channel between the two needs to be analysed. Since communication through such a channel creates many multipath components, finding the location of a tag can be difficult. However, the authors do not examine this problem in the paper. In [5], it is suggested that people could wear passive tag equipped objects such as rings or wristbands and these object can be detected with an RFID reader to calculate total number of victims under rubble. Yet a technical analysis of this idea is not presented in the paper. Exploiting passive RFID tag for finding number of victims have been put forward in [22]. Authors discuss attaching RFID tags inside apartments and keeping resident information in these tags. These tags would also store additional information such as presence of elderly and physically disabled people in a particular apartment. Similarly, a reader outside can collect information stored in these tag in an aftermath of a disaster. Likewise, as with other above mentioned studies, the authors do not investigate passive communication challenges associated with the implementation of proposed approaches or give any technical results.

2.3 Communication Channel Model for Collapsed Building Ruins

One of the main problems that need to be addressed while studying communication between a tag inside ruins and a reader outside, is formulating a suitable communication channel model. Few papers have investigated this issue for UHF band. Authors in [12] describe the total power loss through a channel with ruins equal to the sum of free space path loss and attenuation through medium with construction materials such as concrete, brick, cement. The distribution of these materials in a channel is assumed to be Gaussian. The paper also presents measurement results of wave propagation through brick obstacle to calculate the signal attenuation. However, no measurement is taken to confirm the assumptions used in deriving the model. The channel model presented also does not take into account the losses due to effects of multipath. In contrast, [13] considers the effects of multipath fading for channel model in addition to losses due to obstacles. However, the channel model is based on indoor signal attenuation model given in [23], and therefore, only considers walls as obstacles. As walls are often built using bricks, the model does not fully characterise the total power loss through channel with ruins. [24] gives a model for the communication channel in rubble made of free space communication model given in [25] and attenuation through layers of construction materials. In the paper, measurements are taken through medium made of stratified layers of concrete to verify predictions of the channel model. Even though values obtained in measurements and in mathematical model for the amount of attenuation over a layer of concrete are similar, it is unclear whether this model can describe power loss over a channel in rubble, where concrete and brick obstacles do not stay in layers but are distributed randomly. The study also minimizes the effects of multipath fading, which is a significant contributor to power loss.

Finally, [14] uses autoregressive modelling (AR) for representing communication channel response in building ruins. Measurements are taken through both stratified concrete and chaotic distribution of various construction materials. The authors present a channel simulator based on the results of AR modelling. The channel model is presented in the form of an impulse response, where multipath components are represented with corresponding amplitudes and delays. The paper argues that the amplitudes and delays of multipath components can be characterized as random variables obeying Log-normal and Weibull distributions, respectively. However, the results of AR modelling are based on obtained measurements from small artificial collapses that do not necessarily represent a real collapsed building. Thus, the channel simulator presented in the study can only be useful in cases dealing with small ruins.

2.4 The Use of Other Means for Detecting and Locating People Under Rubble

As search and rescue operations are important to be carried out efficiently, researchers have proposed other ways for finding victims of natural disasters using technology. Methods like using snake-like robots [7, 26], detecting respiratory movements [8, 27, 28], using RADAR systems to locate people [29, 30], detecting cell phones and other RF devices [10, 31–34] and using a helicopter to scatter active RFID-based sensors inside building ruins to detect human features such as voice and heat [9] have been suggested. These studies, however, do not address vital issues such as signal interference and communication channel power loss, and therefore, are not able to provide full system performance analysis based on the obtained results.

Although various approaches have been previously introduced, to the best of our knowledge, this is the first study to propose a disaster recovery system based on passive wireless communication for calculating the total number of victims trapped under a rubble and their possible locations. We model the communication channel under ruins and experimentally validate the derived model. We measure the performance of our system and report the results on feasibility. We also lay out the characteristics of RESCUE reader and sensors.

Chapter 3

SYSTEM ARCHITECTURE

3.1 Overview

RESCUE system architecture is illustrated in Fig. 3.1. It is composed of sensors under rubble and a reader. The sensors are installed inside building during construction. After an earthquake the reader is placed outside ruins to read data that sensors store. During data reading, sensors act as passive devices, using incident RF continuous wave (CW) as an energy source.

Sensors consist of six main modules, i.e., microcontroller, earthquake detector, camera, passive RFID tag, power source and antenna switch as shown in Fig. 3.2. The task of a sensor is to detect occurrence of an earthquake, take images of building interior and communicate that information back to the reader on demand using EPCGlobal Class 1 Generation 2 protocol [35]. The average duration of an earthquake is a about 50 seconds [36]. Thus, we propose that the sensors take pictures of building interior for hundred seconds. In total ten images are taken during this period. The purpose of taking pictures is to be able to identify number of people inside building prior to an

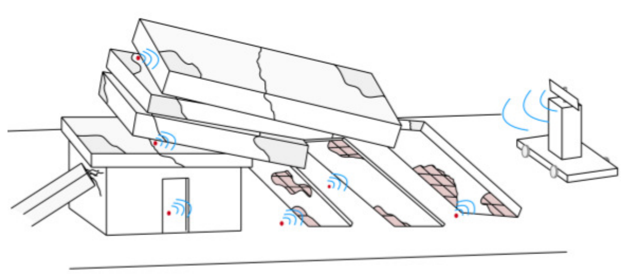

Figure 3.1: System architecture. The reader reads data from sensors under ruins.

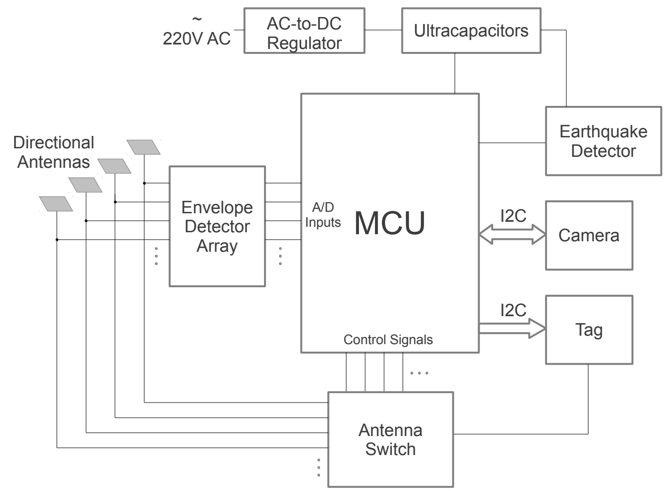

Figure 3.2: Internal circuit diagram of a RESCUE sensor.

earthquake. Therefore, having taken one image every ten seconds, this information can be retrieved.

At the time of an earthquake, earthquake detector module triggers microcontroller. As a result, microcontroller activates camera every ten seconds for hundred seconds to take a picture. Microcontroller and camera communicate through serial I^2C interface [37]. The images are encoded in JPEG format with 8KB image size [38] and saved into RFID tag memory. This is likewise achieved via I^2C interface between microcontroller and passive RFID tag.

Building electrical power is often cut off at the time of an earthquake. Power might also fail due to other reasons such as an accident in city electrical grid or due to circuit breaker as a result of high voltage fluctuations. Therefore, RESCUE sensors should be able to provide reliable functionality even in the temporary absence of external power. For this reason, we propose using small size powerful ultracapacitors to operate microcontroller, earthquake detector, camera and antenna switch. Ultracapacitors are connected to the electrical grid through a AC-to-DC regulator and stay charged throughout the lifespan of a sensor. The main reason that we use ultracapacitors as power source instead of a lithium battery is because ultracapacitors have much larger service time than batteries, in addition to many other advantages [39]. An average life span of a building is 50-60 years, and therefore, a sensor installed inside should have similar lifetime. Ultracapacitors today have only up

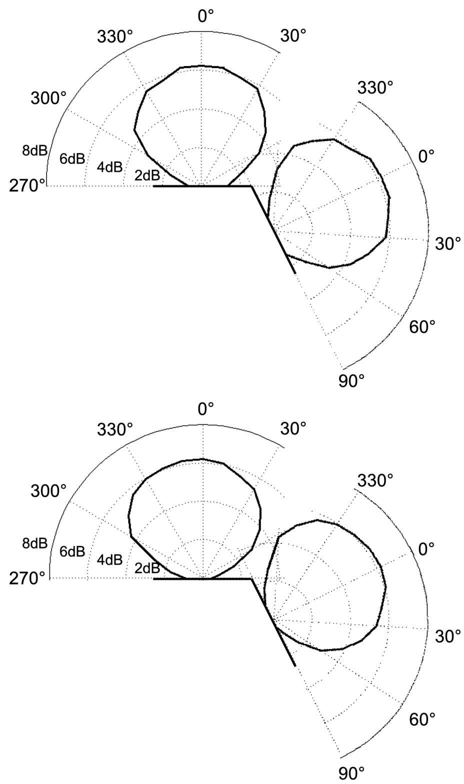

Figure 3.3: Radiation pattern of two faces of a sensor for (a) horizontal and (b) vertical polarizations.

to 20 years of lifetime; however, research is ongoing to increase lifetime of ultracapacitors with the use of carbon nanotubes [40].

At the time of collapse, a sensor can end up at any arbitrary orientation. To guarantee reliable data reading, sensors should be able to communicate with a reader from any direction. One solution is to equip sensors with omnidirectional antennas. However, this eliminates any antenna gain at the sensor. To maximize read range of sensors and minimize reader transmission power, we propose to use an antenna shell around sensors in the shape of polyhedron with a directional antenna attached to each face as shown in Fig. 3.4. Sensor is capable of detecting the direction of the reader and subsequently, uses the antenna directed to the reader. We propose three ways to realize this. In the first method sensor detects the antenna with highest level of incident RF CW and uses that antenna during transmission and reception to maximize sensor EIRP. Using analog-to-digital

(A/D) converter, the output of simple envelop detector shown in Fig. 3.5, microcontroller compares signal levels from directional antennas. The capacitor and resistor values of envelop detector are chosen appropriately to match signal period of $900MHz$ wave and minimize power dissipation. Microcontroller subsequently activates control signal on antenna switch input corresponding to the antenna with highest signal strength, as shown in Fig. 3.2. Fig. 3.3 shows radiation pattern of two adjacent directional antennas of a sensor for horizontal and vertical polarization. Radiation pattern data belongs to Omni-Id Dura 3000 [41] tag antenna. It can be observed that given that the reader signal is coming in the direction of one of the antennas, it will be largely attenuated on adjacent directional antennas. Additionally, there exists many multipath components coming from different directions. Due to high level of clutter in the channel due to ruins we assume that all antennas will have similar level of mean multipath signal power. However, since one of the antennas receives the LOS component of the reader signal, the total receive power level at that antenna will be larger than other antennas. Microcontroller compares the moving average value of power on each antenna and chooses the antenna with highest moving average receive power for the the communication. $MSP430F5328EP$ has total information memory of $144B$. Each sample of the A/D converter of the microcontroller is $12bits$. Therefore, for a dodecahedron (12 faces) shaped sensor, moving average of 20 samples can be used for antenna selection. Antenna switch is able to connect any one of the input signals to output using control inputs. As a result, tag antenna input is connected to the antenna with highest incident RF CW.

Second method consists of equipping sensor with a electronic 3D compass [42]. The reader transmits a static magnetic field such that the strength of this magnetic field surpasses the magnetic field strength of the earth ($\approx 50\mu T$) at the compass location. This will result in compass aligning with the magnetic field of the reader. Using this information sensor chooses the antenna directed at the reader. There are several ways that the reader can generate a magnetic field, such as using a magnet or a wire with a current. With 100 parallel wires stacked together the reader can generate the required magnetic field at $10m$ distance with $25A$ electric current.

In the third method, sampling rate of the A/D converter of the microcontroller installed inside sensor is chosen very high to detect the line-of-sight (LOS) component of the reader signal. Multipath components are received by all antennas of a sensor with some delay. Given that a sensor has high enough sampling rate, it can the LOS component of the reader signal, which is received first. The antennas of a sensor may receive multipath components of the reader signal at the time when reader is communicating with another sensor. To guarantee a reliable detection of LOS component, a sensor may start analysing received signals on the antennas when the reader sends a command to read a new sensor. Microcontroller the reader command through tag-microcontroller interface. According to data from [14] the first arrival time of multipath components inn $900MHz$ band can be as low as $2.5ns$. This requires a sampling rate of $1Gsps$. Current chips with such sampling rate consume large amount of power. This method can be feasible as power consumption of processors are reduced. Carbon nanotube based chip designs [43] show promising results.

The model of each component that can be used in the RESCUE sensor is given in Table 3.1. Two ultracapacitors power separate parts of a sensor. Minimum operating voltage for earthquake detector, camera, microcontroller and antenna switch are given in Table 3.2. Earthquake detector is connected to $VEC5R0755QG$ ultracapacitor, which can provides $5V$ ($3.3V$ through a voltage regulator [44]) and has $7.5F$ capacitance and the other components power up from $VEC3R0507QA$, ultracapacitor with $3V$ rated voltage and $500F$ capacitance. The total available energy inside ultracapacitor can be calculated as [45]

$$E = \frac{1}{2}C(V_{initial} - V_{min})^2 \tag{3.1}$$

where C is capacitance, $V_{initial}$ the initial voltage of the ultracapacitor and V_{min} is the minimum operating voltage of the component being fed.

According to Table 3.2, $VEC5R0755QG$ can feed earthquake detector for 9.5 $days$ without an external power. Before an earthquake, microcontroller is in the standby mode. Earthquake detector triggers microcontroller at the time of an earthquake, and as a result, microcontroller switches to active mode. Microcontroller stays in the active mode until ultracapacitor energy can no longer provide the required operating voltage. Similarly, taking into account voltage requirements of microcontroller, camera and antenna switch along with power requirements in Table 3.2, it can be calculated using (3.1) that the sensor can stay functional for approximately 14 $hours$. As it can be seen in the performance evaluation in Chapter 5, this period is sufficient for successful data collection from sensors.

Table 3.1: Example models of the RESCUE sensor components.

Component	Model
$Microcontroller$	$MSP430F5328 - EP$ [46]
$Earthquake\ Detector$	$Model\ 832\ Accelerometer$ [47]
$Camera$	$TCM8230MD$ [48]
$Passive\ RFID\ Tag$	$TegoChip$ [49]
$Ultracapacitors$	$VEC5R0755QG$, $VEC3R0507QA$ [50] [51]
$AC - to - DC\ regulator$	$MAX610$ [52]
$Antenna\ Switch$	$6 \times ADG787$ [53]

Table 3.2: Power requirements of sensor components.

Component	Power Requirement	Minimum Supply Voltage
$Microcontroller$	$7mW$	$1.8V$
$Earthquake\ Detector$	$13.2\mu W$	$3.3V$
$Camera$	$53mW$	$2.6V$
$Antenna\ Switch$	$0.6\mu W$	$1.8V$

After reader collects data from sensors, using an automatic human detection algorithm or a manual operator, it is possible to identify the number of people on each image and therefore under ruins. Furthermore, the locations of people in the building just before earthquake can be determined, which can aid rescue workers in finding victim locations.

3.2 RESCUE Data Collection

The main criteria to consider when deciding reader location for data collection is minimization of power loss between RESCUE reader and sensors. Reader placed to one location to read data from sensors might have low power loss to some sensors while having very high power loss to the others. In such case, reader needs to have very high transmission power to read all sensors located under ruins. To overcome this problem, we propose that the reader is moved around the rubble such that it can read data from all sensors, and therefore, require lower transmission power.

Adjusting distance of reader from rubble during data collection is critical. Even though placing the

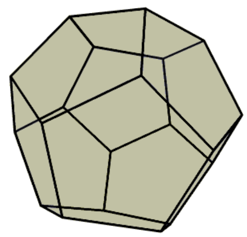

Figure 3.4: A RESCUE sensor shape.

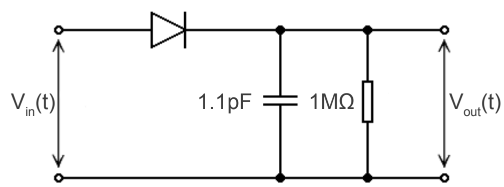

Figure 3.5: Simple signal envelope detector.

reader close to the ruins decreases power loss, at the same time, it poses other problems. Firstly, parts of rubble usually cover some space in front of a building, and therefore, the reader cannot be easily moved around the area. Secondly, when the reader approaches the building too much, concrete floors start to dominate the medium between reader and sensors on higher floors. Thus, power loss, as well as required transmission power increases.

In this study, first we carry out simulation of data collection to determine required reader transmission power and resulting total duration of data collection from sensors. During simulations, on each step while reader is moving around rubble, power loss between each sensor and reader is calculated and stored. Afterwards, among these evaluated values an algorithm notes the minimum power loss value and corresponding read location for each sensor. Finally, transmission power for a reader is evaluated using calculated power loss values.

On a real situation, it is not possible to calculate the minimum power loss locations for sensor a priori. For this reason, while moving around rubble, the reader can periodically attempt to read data from sensors. Sensors that are activated respond and try to participate in the reading. Sensors have to reflect sufficient power so that the reader received signal level is larger than the reader sensitivity threshold. As soon as the reader receives a response from a sensor, it may stop moving and read data stored on the sensor.

3.3 UHF RFID EPC-Class 1 Generation 2 Protocol

The RESCUE uses EPCGlobal Class 1 Generation 2 (C1Gen2) protocol [35] to read data from sensors. C1Gen2 is widely used RFID protocol for long range passive tags operating in UHF band. Therefore, it is a suitable option to use for reading sensors under ruins. The protocol has two layers, namely physical and MAC layers.

In the physical layer, downlink communication is achieved by the reader using Amplitude Shift Keying (ASK) modulation and Pulse Interval Encoding (PIE) to transmit data. By varying the PIE duration, the reader can control downlink data rate. In the uplink, sensors use backscatter transmission to communicate with the reader. For this, sensors control how well they reflect incident RF continuous wave (CW). Depending on the parameters such as the strength of CW, the reader sensitivity and power loss between a sensor and the reader, read range of a sensor may change dramatically. There are 4 data encoding schemes for sensors that differ in number of cycles, between one and eight. Even though data rate falls with higher number of cycles, communication BER improves as the number of cycles increase.

MAC layer of Gen2 protocol is similar to Framed Aloha protocol [54], where sensors do not hear each other because they transmit at different time frames. As a result, sensors only respond to the reader commands. Sensors contain three memory banks namely, RFU, EPC, TID and $UserMemory$. To read sensors, the reader first transmits a $Select$ command where it specifies which memory bank data will be requested during when sending access commands by setting $11th$ and $12th$ bits appropriately, according to the protocol. To read $UserMemory$, the reader sets both bits to 1. Activated sensors respond to the reader command. Next, the reader sends a $Query$ command specifying which group of sensors shall participate in reading such as sensors with specific $inventoried$ or SL flags. $Query$ command also specifies a Q number to indicate the maximum number of slots that will be used in the inventory round, which equals to 2^Q. Having received the command each sensor randomly chooses a slot number in the range $(0, 2^Q)$. A sensor with slot number zero replies to the command. After reading the sensor that has replied, the reader sends $QueryRepeat$ command. After receiving the command, the rest of the sensors that are activated decrement their slot number and sensor that has slot number zero replies. If a sensor responds, the reader stays in its place to read it, otherwise, the reader moves to detect and read other sensors under ruins.

Sensors transition between five steps during reading. Before receiving $Query$ command, all sensors are in $Ready$ state. After choosing a slot number sensors transition to $Arbitrate$ state and the sensor with slot number zero transitions to $Reply$ state, backscattering a 16-bit number $RN16$ that the reader uses as a handle to target the sensor. In this state, the sensor waits for an ACK from the reader and after receiving a valid ACK, transitions to $Acknowledged$ state. A sensor in the $Acknowledged$ state transitions to $Open$ or $Secured$ state, depending whether it has an access password, upon receiving Req_RN command from the reader. After this, the reader is able to send access commands to the sensor.

The reader accesses each sensor separately on different time frames. Therefore, it is important that the sensor that is not currently being accessed should not stay in a state where it can interfere with other sensors. Thus, if the sensor does not receive a command from reader within specified timeout durations while in $Ready$ or $Acknowledged$, it returns to $Arbitrate$ state and sets its slot number to zero. As soon as the reader issues next $QueryRepeat$ command, it decrements its slot number from 0000_h to $7FFF_h$. The reader has to start a new query round in order to read this sensor.

While in the $Open$ or $Secured$ state, if a sensor receives either $Query$ or $QueryRepeat$, command it transitions its inventoried flag from $A \rightarrow B$ or $B \rightarrow A$. Thus, once a sensor is read, it does not reply to any further command sent by the reader unless the reader issues a new $Select$ command with reverted $inventoried$ flag. As a result, if the reader receives a wrong $RN16$ from a sensor due to channel bit error and thus unable to send an a valid ACK within timeout duration, it may start a new query round for only unread sensors.

3.4 Extended RFIDSim Simulator

RFIDSim [16] is a software that can simulate communication between an RFID reader and passive tags. Parameters of communication can be configured and the simulator produces log files that show all message exchanges between two sides, as well as total runtime of reading process. However, reader element inside RFIDSim lacks some of the features of an actual passive RFID reader. We extended the simulator to include two more capabilities to reader module.

The first addition made was to be able to read data from tag in more than one round. Once a tag enters $Open$ or $Secured$ state, reader should be able to send any number of access commands according to C1Gen2 protocol. The simulator however, only lets a reader send one access command for each run, and thus in order to read all the data on tag reader needs to request whole memory chunk at once. It is beneficial for a reader to be able to access data on tag piece by piece by sending number of $Read$ commands. This is because as BER of a channel increases, reader needs to request smaller amount of data from tag in each $Read$ command in order to increase throughput. Secondly, when tag sends data to reader, it includes a 16-bit checksum at the end of data. Since tag does not change state after it responds to a $Read$ command, when checksum of a received data from a tag is incorrect, reader should be able to request the same data piece again. This feature is not included in RFIDSim. Thus, we have added this feature to guarantee successfully reading all the data stored on tag's memory even if intermediate errors happen[1].

Without these modification, it is hard to predict total read time of tags in our channel.

[1]The extended simulator is available for download from http://nwcl.ku.edu.tr/repository/ExtendedRFIDSim.zip.

Chapter 4

CHANNEL MODEL FOR PASSIVE WIRELESS COMMUNICATION OVER RUINS

In this chapter, we characterize the channel model that we develop. First, we state power loss expression and derive channel error probability. Next, we describe the building collapse simulator, and explain how it is used to calculate power loss between the reader and the sensors. Finally, required reader transmission power is discussed and equations are given.

4.1 Power Loss

Power loss is mainly due to path loss and shadow fading components. Hence, using a modified form of simplified path loss model [55], the power loss in the logarithmic scale is expressed as

$$PL(dBm) = -20log(\frac{c}{4\pi f d_0}) + 10\gamma log(\frac{d}{d_0}) + L_{SHDW} \tag{4.1}$$

where f is the signal frequency, c is the speed of light, d_0 is reference distance, d is the distance between reader and sensor, γ is path loss exponent and L_{SHDW} is the power loss due to shadowing. Since shadowing represents a portion of a signal that does not pass through a certain medium, it can be represented by the transmission coefficient of a medium that signal is passing through. Given that there exist n obstacles between reader and sensors, shadow loss can be calculated as

$$L_{SHDW} = \sum_{i=1}^{n} -20logT_i \tag{4.2}$$

where T_i is a transmission coefficient of i'th obstacle in a medium between the reader and the sensor. Transmission coefficient of a material with permittivity ϵ and conductivity σ can be modeled as a

Table 4.1: Electromagnetic properties of constuction materials.

Medium	ϵ_r	$\sigma\ (S/m)$
$Reinforced\,Concrete$	6.5	0.07
$Brick$	4.5	0.03
$Wood$	3	0.005

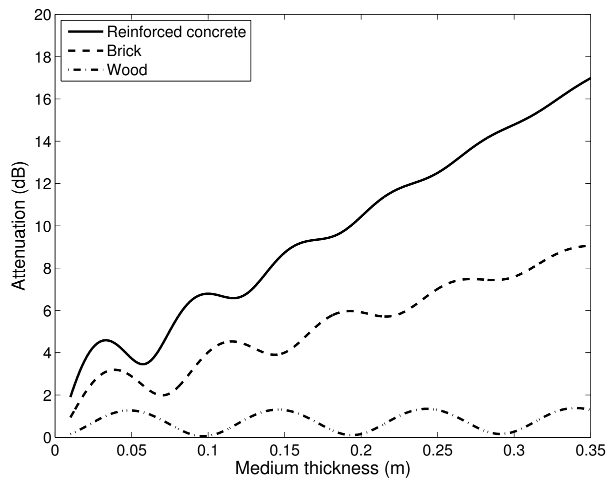

Figure 4.1: Attenuation through mediums as a function of thickness at 866MHz.

three layer medium (air-material-air) and the transmission coefficient for such a medium is given by [56]

$$T = \frac{4}{(1 - Z_{12})(1 - Z_{23})e^{-\gamma_2 d} + (1 + Z_{12})(1 + Z_{23})e^{\gamma_2 d}} \tag{4.3}$$

and

$$\begin{aligned} Z_{ij} &= \frac{\mu_i \gamma_j}{\mu_j \gamma_i} \qquad i, j = 1, 2, 3 \\ \gamma_k &= \pm\sqrt{jw\mu_k(\sigma_k + jw\epsilon_k)} \end{aligned} \tag{4.4}$$

where d is depth of the medium, μ is magnetic permeability, ω is angular velocity and γ is the complex propagation constant. Table 4.1 shows electrical properties of concrete, brick and wood.

Using (4.2), (4.3) and (4.4), we evaluate shadowing of construction materials in Table 4.1 for varying thickness in Fig. 4.1. Calculated attenuation values are in agreement with the results reported in other studies [57–59]. As it can be observed, shadowing through wood is much less than that of concrete and brick. For this reason, we have eliminated wooden materials from our calculations for this study.

Since the channel between the reader and the sensors contains many obstacles, this creates many multipath components. However, because sensors are equipped with directional antennas, most of the multipath components coming from different directions are eliminated. Therefore, there is a dominant LOS component between the reader and the sensors. Consequently, we assume that the communication channel exhibits multipath Rician fading [60].

4.2 Channel Error Probability

To the best of our knowledge, there is no closed form expression for BER in a Rician fading RFID communication channel. Average BER for a rician fading channel can be calculated using

$$P_e = \int_0^\infty P_b(\gamma) f_\gamma(\gamma)\, d\gamma \tag{4.5}$$

where $P_b(\gamma)$ is probability of error in an AWGN channel and f_γ is the distribution density for Rician distribution. BER in an AWGN channel for RFID communication can be obtained from [61]

$$P_b = 2Q(\sqrt{M\gamma})[1 - Q(\sqrt{M\gamma})] \tag{4.6}$$

where $Q(x)$ is the Q-function and M is number of cycles in tag's data encoding scheme. Rician fading probability distribution is given as [62]

$$f_\gamma(\gamma) = \frac{(K+1)}{\overline{\gamma}} exp\left[- K - \frac{\gamma(K+1)}{\overline{\gamma}} \right] I_0 \left[2\sqrt{\frac{\gamma K(K+1)}{\overline{\gamma}}} \right]$$

where $\overline{\gamma}$ is average effective SNR, K is the ratio between dominant signal component and other multipath components, and $I_0(x)$ is the first kind and zero-order Bessel function.

We solved the integral in (4.5) by employing Gaussian-Legendre quadrature [63] numerical integration method. The integral can be expressed as

$$P_e = \int_0^{\gamma\prime} P_b(\gamma) f_\gamma(\gamma)\, d\gamma \tag{4.7}$$

where $\gamma\prime$ is a large number. By rearranging (4.7), using $\gamma = a \cdot x + c$ and taking the range of x as [-1,1], such that $a = \frac{\gamma\prime}{2}$ and $c = \frac{\gamma\prime}{2}$,

$$\begin{aligned} P_e &= \frac{\gamma\prime}{2} \int_{-1}^{1} P_b(\frac{\gamma\prime}{2}x + \frac{\gamma\prime}{2}) f_\gamma(\frac{\gamma\prime}{2}x + \frac{\gamma\prime}{2})\, dx \\ &\approx \frac{\gamma\prime}{2} \sum_{i=1}^{n} w_i P_b(\frac{\gamma\prime}{2}x_i + \frac{\gamma\prime}{2}) f_\gamma(\frac{\gamma\prime}{2}x_i + \frac{\gamma\prime}{2}) \end{aligned} \tag{4.8}$$

and

$$w_i = \frac{2}{(1 - x_i^2)(P_n(x_i))^2} \tag{4.9}$$

using Gaussian quadrature method, where n is the number of points used for numerical calculation, w_i is i'th point's weight coefficient and $P_n(x)$ is a Legendre polynomial, which can be expressed using Rodrigues' formula [64] as

$$P_n(x) = \frac{1}{2^n n!} \frac{\mathrm{d}^n}{\mathrm{d}x^n} \left[(x^2 - 1)^n \right] \tag{4.10}$$

Using (4.8), we evaluate BER in the channel between the RESCUE reader and sensors. BER is then used to obtain total read time of data inside RESCUE sensors.

4.3 Building Collapse Model

The building collapse model is based on ASI-Gauss [15] technique that is applicable for seismic collapse analyses of framed structures. The technique can simulate dynamic behaviors of large-scale framed structures with strong non-linearities and discontinuities. Isobe Lab research group at University of Tsukuba has developed this technique and has also released seismic collapse analysis simulator that can be used to construct structures and apply the proposed technique. We have used

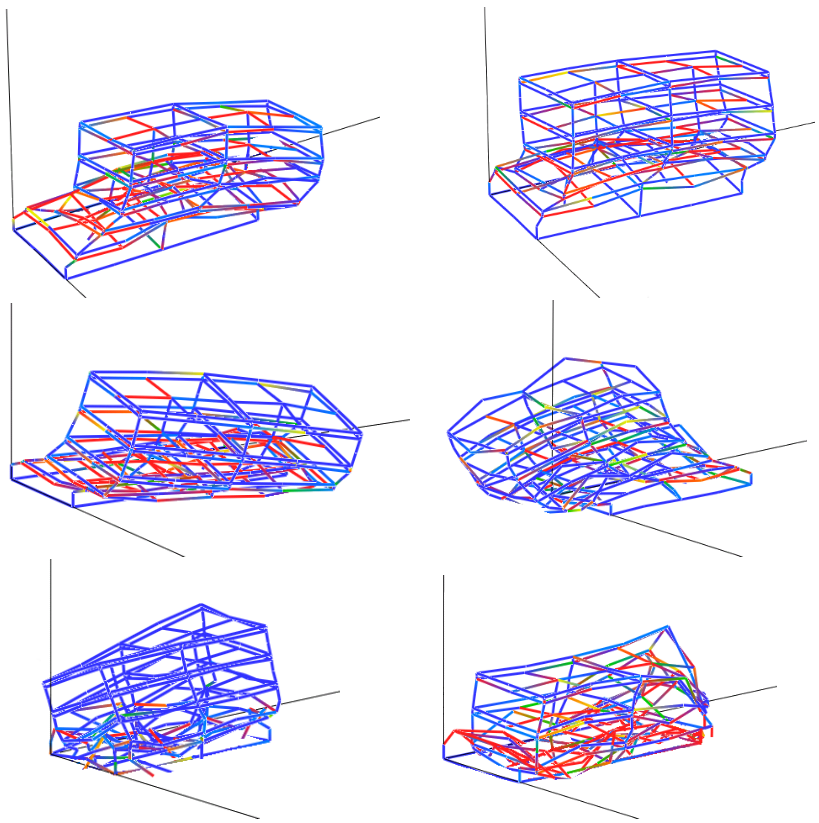

Figure 4.2: Simulated six different collapse scenarios.

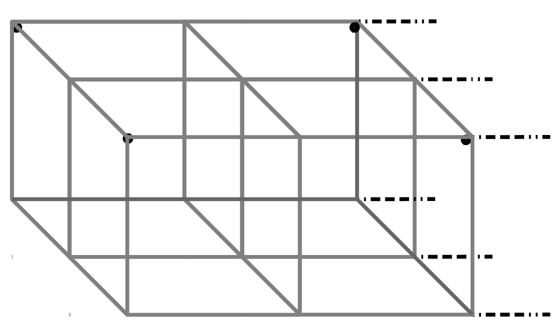

Figure 4.3: An apartment in a building. Sensor locations are shown in black dots.

this simulator for our study. The magnitude of the applied earthquake have been set high in order to make the structure collapse.

The structure we have built for this study has five storeys, with two apartments on each storey. Each apartment is made of four rooms. The overall dimensions of the constructed structure model are (8m)x(16m)x(12m). We have carried out seismic collapse analyses on the structure by varying parameters and have obtained six different kind of collapses that might occur as a result of a destructive earthquake. Fig. 4.2 shows six possible post earthquake scenarios. These collapses are used for performance evaluation of RESCUE.

Fig. 4.3 shows placement of sensors in an apartment of a building. There is one sensor per room and they are shown in black dots. The sensors are assumed to stay attached to the same corners of rooms after building collapse.

4.4 Communication Medium Model

To evaluate the total power loss between reader and sensors, medium assessment between them needs to be performed. For the channel being considered, in addition to path loss and multipath fading, there is a signal strength loss resulting from building ruins present along the link between reader and sensors. This loss is characterized as shadow fading, and plays a significant role in determining overall power loss present in the channel. Therefore, to correctly carry out received power calculations, it is imperative to describe the channel in terms of materials present along the communication link.

Using the building collapse simulator software, we construct a framed structure with the use of beams. The software can only simulate an earthquake on framed structures. Therefore, the simulated building does not contain any walls, floors and ceilings. Since durability of a building also depends also on those parts, we add additional beams to corresponding locations to increase endurance.

We assume that the framed structure does actually have walls and ceilings. Supposed locations of walls and ceilings are noted using coordinates of surrounding four corner joints in the framed structure. At the end of a simulation, the software outputs the final coordinates of all the joints of the structure. Using this data, final locations of all the supposed walls and ceilings are evaluated and used to evaluate the media between a sensor under rubble and a reader outside ruins.

To obtain the media in between, we divide direct line separating a reader and a sensor into large number of discrete points. Each of the points is classified as being inside a concrete slab, brick wall or in free space. Then, by adding number of points inside each medium type separately, approximate amounts of concrete, brick and free space in the channel are captured.

Concrete slabs and brick walls inside the rubble are considered as individual cuboids. We propose a technique to determine whether a point in three dimensional space is inside any of the existing cuboid volumes, using cuboid coordinates. In Fig. 4.4, a cuboid in shown. $ABCD$ is a rectangle that lies on a plane, parallel to and located in the middle of upper and lower surfaces of the cuboid. Given such a cuboid and a point $P(x, y, z)$ in a three dimensional space as shown in the figure, it is possible to analytically determine whether the point is inside the cuboid. To achieve this, two conditions need to be satisfied. First, distance from the point to the plane that $ABCD$ is located on should be calculated. If the distance is the lower than $h/2$, where h is the height of the cuboid, then the second condition should be checked. For the second condition, θ angles need to be evaluated using

$$\theta_A = acos\left(\frac{(\vec{AB} \times \vec{AP}) \cdot \vec{n}}{|\vec{AB} \times \vec{AP}|}\right)$$
$$\theta_B = acos\left(\frac{(\vec{BC} \times \vec{BP}) \cdot \vec{n}}{|\vec{BC} \times \vec{BP}|}\right)$$
$$\theta_C = acos\left(\frac{(\vec{CD} \times \vec{CP}) \cdot \vec{n}}{|\vec{CD} \times \vec{CP}|}\right)$$
$$\theta_D = acos\left(\frac{(\vec{DA} \times \vec{DP}) \cdot \vec{n}}{|\vec{DA} \times \vec{DP}|}\right)$$

where $\vec{n}$ is the normal vector of the plane that $ABCD$ lies on. If all four θ values are smaller than $\pi/2$ or bigger than $\pi/2$ at the same time, then, the point is inside the cuboid. Otherwise, the point is located outside the cuboid.

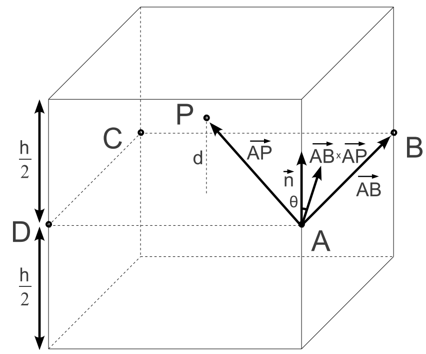

Figure 4.4: A cuboid and an arbitrary point P in three dimensional space.

4.5 Reader Transmission Power

One of the main aims of this study is to determine appropriate reader transmission power for the reader. To successfully read data from a passive sensor, two conditions need to be satisfied. Firstly, sensor received power should be higher than the activation power of sensor RFID tag to turn on. Secondly, power reflected from a sensor has to be high enough to cross reader sensitivity level. By combining these two conditions, the required minimum reader transmission power to read data from a sensor is expressed as

$$P_{TXmin}(dBm) = \max\Bigg[\Big(P_{RS} + 2PL - 2(G_R + G_T) -20log(\rho)\Big),\ \Big(P_{ac} + PL - (G_R + G_T)\Big)\Bigg] \quad (4.11)$$

where P_{RS} is reader sensitivity, PL is power loss between reader and sensor, G_R and G_T are antenna gains of reader and sensor respectively, ρ and P_{ac} are sensor RFID tag backscatter power ratio and activation power respectively. Reader received signal SNR can be evaluated as [65]

$$SNR = P_{RDrec} - NF(dB) - 10log(BW) + 174 \quad (4.12)$$

where P_{RDrec} is the reader received signal power, NF is the noise factor, BW is the total bandwidth of the receiver and -174 is the effective noise power available in $1Hz$ bandwidth at $290K$ temperature. P_{RDrec} can be expressed by

$$P_{RDrec} = P_{TXmin} - 2PL + 2(G_R + G_T) + 20log(\rho) \tag{4.13}$$

In the performance evaluation chapter, in Fig. 5.4, we show the dependence of a reader received signal SNR on read time of a sensor data. As SNR increases, time spent to access data from a sensor decreases. However, such correlation does not continue further after approximately $30dB$ SNR. Therefore, we evaluate the data collection performance by increasing reader transmission power, until $30dB$ SNR is reached.

In our simulations of building collapse, we examine only one five storey building subject to six different earthquakes. To calculate required transmission power higher storey buildings, we use shadow fading distributions of five storey collapsed building. We assume that the percentage of both concrete and brick in the channel are similar in ruins of five storey and higher storey buildings. The dimensions of the rubble of various storey buildings [66] are used to evaluate total power loss in the channel.

Chapter 5

PERFORMANCE EVALUATION

In this chapter, we evaluate the performance of the proposed RESCUE architecture. We aim to determine total read duration and transmission power for optimal performance. We use two simulators for performance estimation. Extended RFIDSim simulator was used for read time calculations. MATLAB was used for channel content, power loss and transmission power calculations. We analyze how channel BER affects the results.

5.1 Power Loss

As mentioned previously, a simulation is carried out to derive channel content to every sensor from each reader location. Using channel content, total power loss is calculated by (4.1). Finally, minimum of calculated values for each sensor is selected as power loss between reader and sensor.

For calculation of channel content, concrete width, brick wall width and the number discrete points that link between reader and sensor is divided to are $30cm$, $15cm$ and 10^5, respectively. The rest of the parameters are as following: $f = 866MHz, d_0 = 0.5m, \gamma = 4$. The frequency was selected to match the frequency at which experimental study was conducted. d_0 and γ values were chosen considering channel density.

There are 4 sensors in each apartment and 10 apartment in the 5 story building. The distribution of the lowest power loss values is given in Fig. 5.1. The figure represents power loss values from all 6 collapse scenarios. As a result, in total number 240 power loss values are represented in the graph. The lowest value for power loss is around $45dB$ and highest value is close to $90dB$. The highest distribution of values is between $65dB$ and $85dB$.

The reader stays $3m$ away from the rubble at all times, and its antenna is circularly polarized.

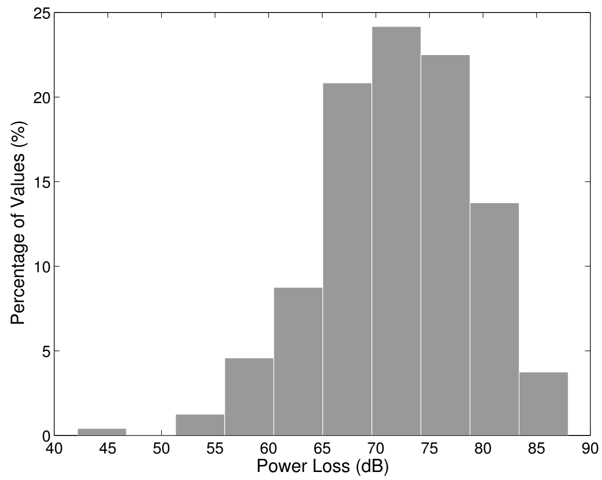

Figure 5.1: Distribution of minimum power loss values for 6 different collapse scenarios.

Table 5.1: RFIDSim simulation parameters.

Parameter	**Value**
$Reader\ Tari\ value$	$25\mu s\ (\approx 32kbps)$
$MAC\ layer\ delays$	$None$
$Tag\ backscatter\ ratio$	15%
$Reader\ antenna\ gain$	$13dB$
$Tag\ antenna\ gain$	$10dB$
$Operation\ frequency$	$866Mhz$
$Background\ noise$	$-100dBm$
$Noise\ Factor$	$22dB$
$Receiver\ bandwidth$	$1.6MHz$
$Temperature$	$290K(=16.85°C)$
$Reader\ sensitivity$	$-90dBm$
$Tag\ sensitivity$	$-18dBm$

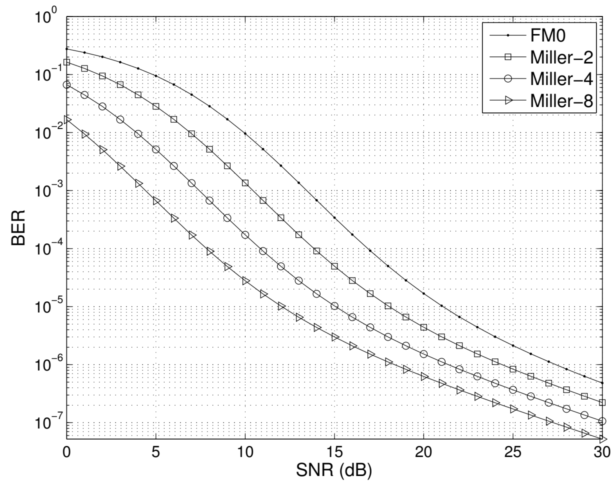

Figure 5.2: Bit-error-rate for different tag data encoding schemes in RFID Rician fading channel.

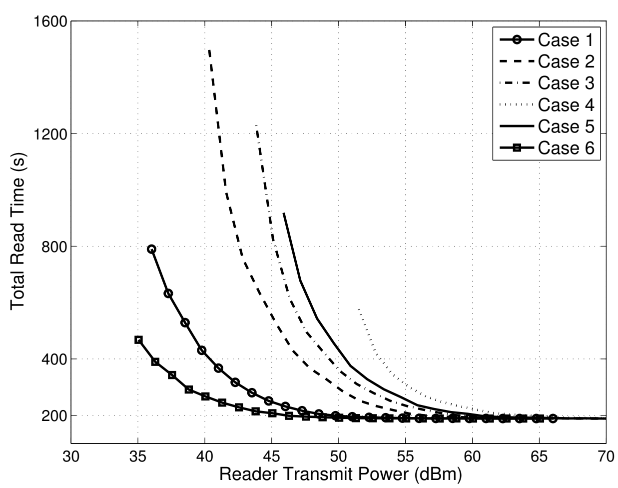

Figure 5.3: Total read time of one images from forty sensors under ruins vs. reader transmission power.

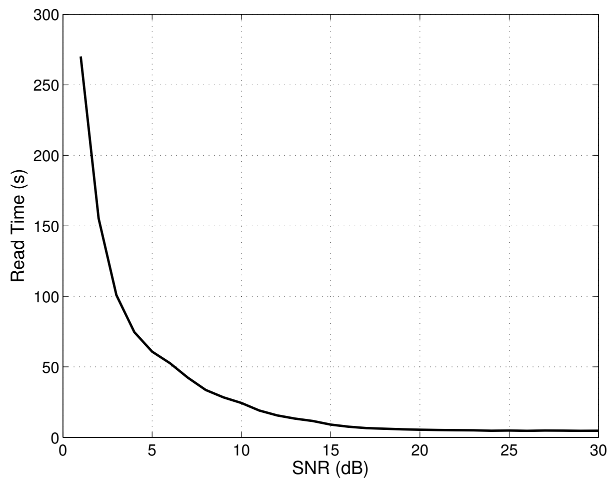

Figure 5.4: Dependence of read time on SNR for 8KB data reading.

5.2 Read Time and Transmission Power

Parameters used during simulation are given in Table 5.1. In the experimental part, we use Omni-ID Dura 3000 tag. Activation power of the tag is $-20dBm$. Free space read range of this tag is 35 meters with $30dBm$ transmit power. Using this information, tag antenna gain can be calculated to be $12dB$. Since power coming from the antennas also passes from the envelope detector of a sensor, some of the energy is dissipated on the envelope detector resistors. Therefore, we take sensor antenna gains to be $10dB$. Tag activation power level is much higher than noise level. Additionally, since length of data that reader sends is short, we neglect bit-errors on tag's side. Reader sensitivity is taken as $-80dBm$. There is a commercially available reader with this sensitivity [67].

Channel BER is evaluated using (4.8). To numerically calculate channel error probability, 5 points were used. $\gamma\prime$ is taken as 10^5 and Rician fading parameter is taken as $K = 10$. The resulting BER values are shown in Fig. 5.2. Each curve corresponds to a different cycle number (M) that represent 4 data encoding schemes.

The total time spent by reader transmitting power to read one image from all 40 tags is evaluated using RFIDsim simulation and is shown in Fig. 5.3. The figure displays results for all 6 collapse scenarios. It can be observed that for high transmit power levels read time for all cases does not decrease further from approximately 20 seconds. Since reader BER decreases with increasing received SNR, the amount of retransmissions decrease as well. This results in similar read times. This is best illustrated in Fig. 5.4. It should also be noted that total read time is directly proportional to the amount of data reader requests from sensors. As a result, if reader chooses to read higher number of images stored in sensor' memory, read time increases as much. When calculating total read time, we exclude times at which no sensor responds to reader $Query$ command. Even though reader transmits power during this period, duration is in the order of milliseconds, which is short in comparison.

One of the parameters of a $Read$ command is the word size of the data to be requested from a sensor. It is an important parameter because depending on receiver BER, read time of a sensor may dramatically change. Another parameter that affects read time is tag data encoding cycle number. As shown in Fig. 5.2, each SNR value corresponds to 4 different BER values. As cycle number increases from $FM0$ to $Miller-8$, the duration of each bit during backscattering doubles. Longer duration results in fewer bit-errors. Therefore, there exists a trade-off between deceasing total read time and minimizing BER. Fig. 5.5 shows read time of one sensor for 4 different M and BER values. When calculating total read time shown Fig. 5.3, we pick the most optimal word size and cycle number for every request, depending on reader SNR. Even though M is specified during $Query$ command, in order to set optimal M, reader can send a second $Query$ command by taking into account SNR of the first sensor response signal.

For the data shown in Fig. 5.3, time axis represents the total time spent by reader to read all data on all sensors. With lower power levels, sensors under ruins can be partially read. The total time spent and transmitted power level to read data from only certain percentage of tags are given in Fig. 5.10. As reader transmission power increases, the number of sensors that can be read increases as well. In the figure, the reading of a new sensor results in increase in the read time. As the transmission power increases further, the total read time starts to decrease until another sensor is read. This is similarly due to the fact that SNR increases with the transmission power, which decreases total read time.

Fig. 5.3 represents the read time and transmission power for collapsed 5 storey building. To determine the required transmission power for various storey buildings, we use simulation data from

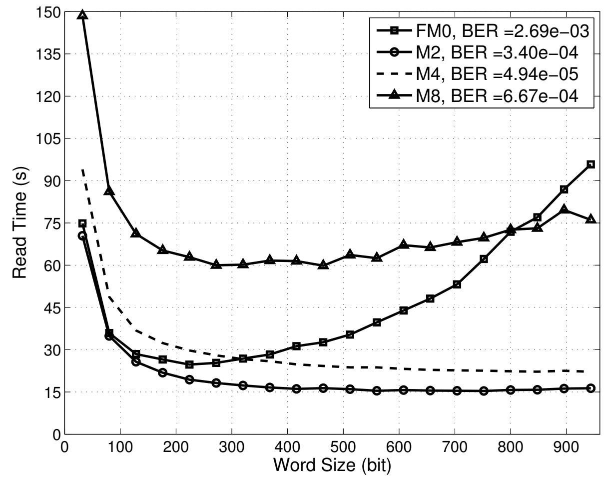

Figure 5.5: Read time for different word sizes and tag data encoding schemes.

simulated 5 storey building collapse. One of the main components of power loss in the channel is shadowing. Fig. 5.6 and Fig. 5.7 show the fraction of concrete and brick in the channel for the simulated 5 storey building collapses. We use concrete and brick fraction corresponding to $0.9CDF$ to evaluate maximum transmission power that is needed to read all the sensors under ruins. Fig. 5.8 illustrates calculated transmission power levels and read times to access one image from one sensor for building sizes ranging from 2 to 20 storeys.

Fig. 5.9 shows average data rate in tag-reader communication with increasing SNR. Data rate starts to saturate around $135kbps$ at $30dB$ SNR, similarly due to decrease in BER.

Even though reader transmission power levels as shown in Fig. 5.8 are much higher ($10W - 1MW$) than allowed $2W$ EIRP in Europe and $4W$ EIRP in US by regulations in UHF band, proposed reader is to be used only for emergency disaster recovery operations for a short period of time.

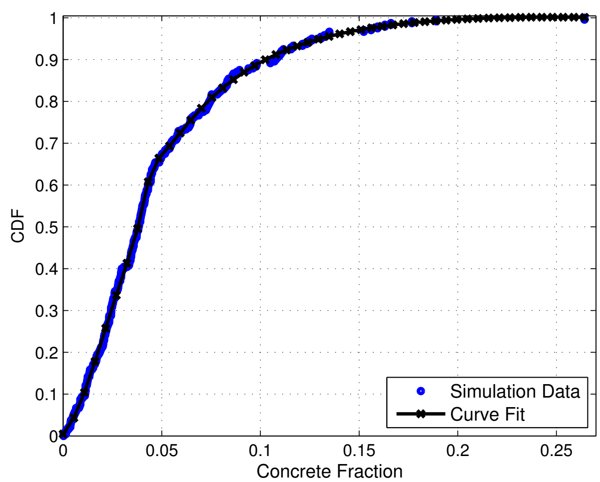

Figure 5.6: The distribution of fraction of concrete in the channel between reader and sensors under ruins.

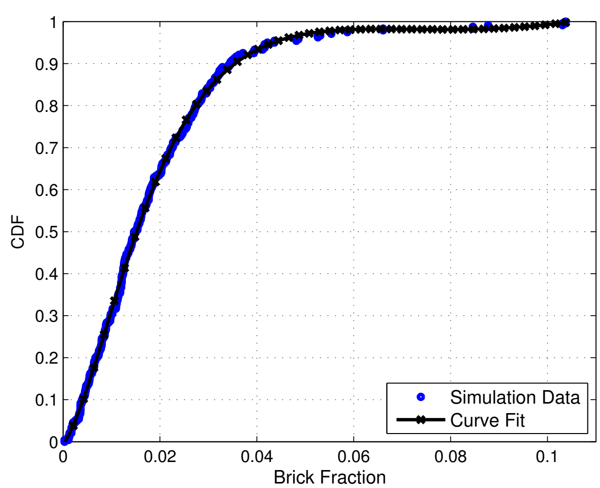

Figure 5.7: The distribution of fraction of brick in the channel between reader and sensors under ruins.

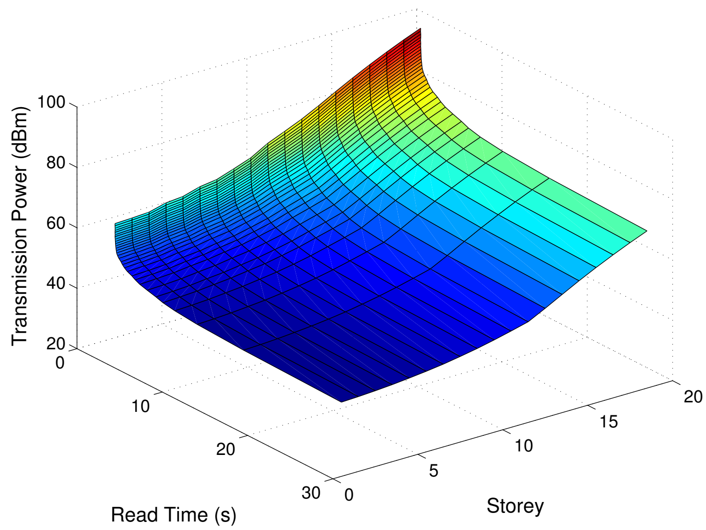

Figure 5.8: Reader transmission power with read time of one image from one sensor for buildings of 2-20 storeys.

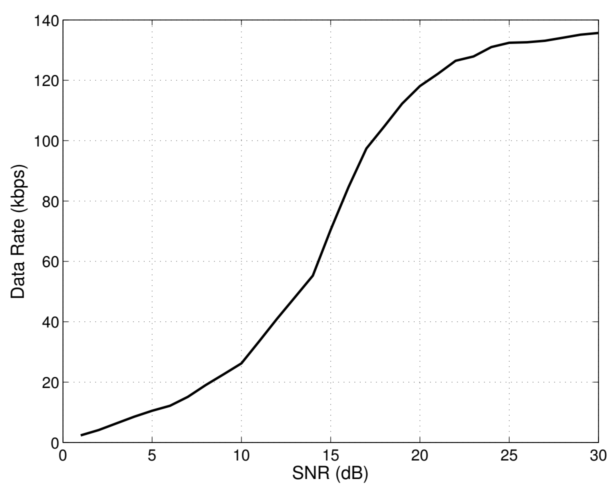

Figure 5.9: Average data rate during backscattering for different SNR values.

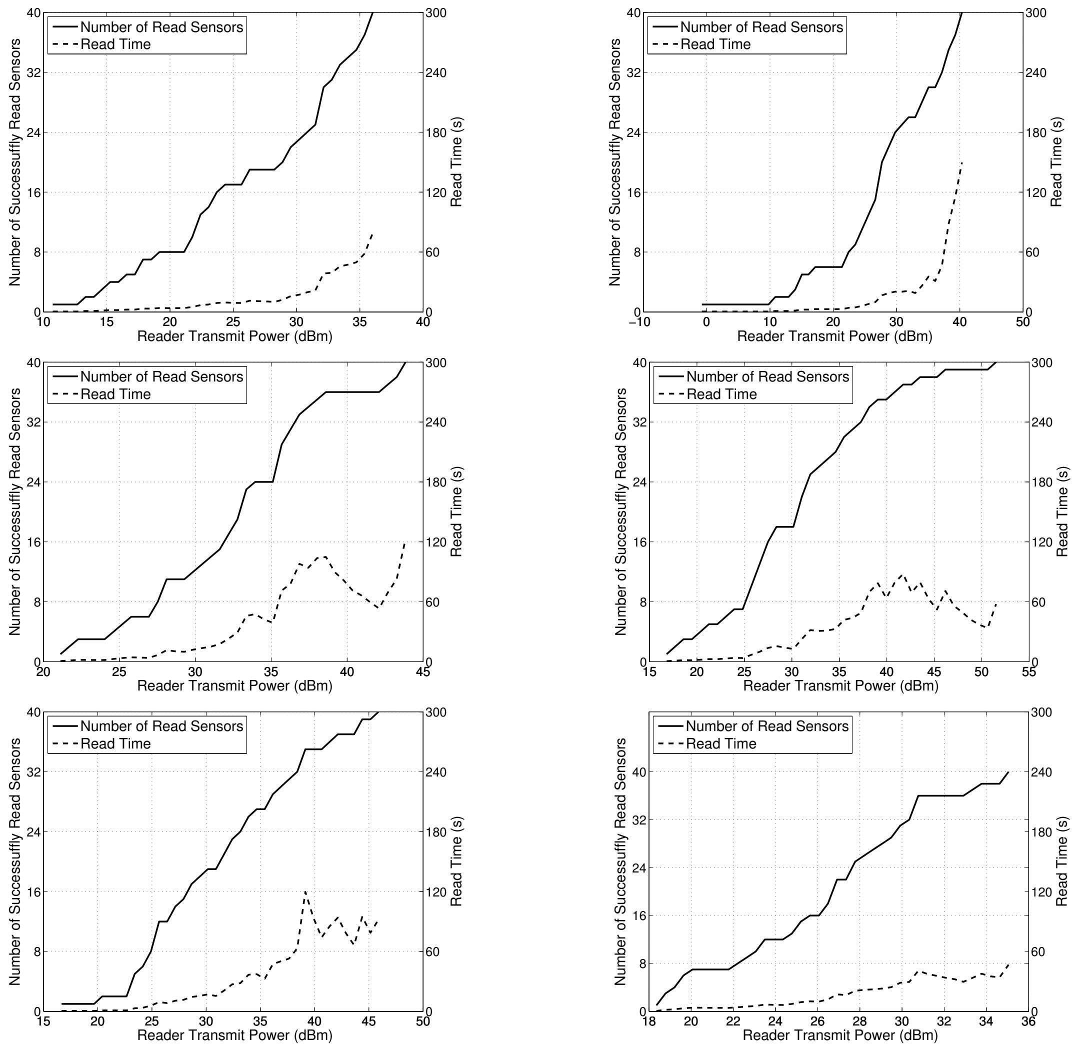

Figure 5.10: Total read time of partial reading of tags under ruins for all six cases.

Chapter 6

EXPERIMENTAL RESULTS

In this chapter, we present the details of the experimental study. First, we describe all hardware and software tools that have been used to realize the experiment. Then, we specify the details of experimental setup, and how the experiment have been carried out. Finally, we give results obtained.

The are two main goals in the experimental study. The first goal is to read data on passive RFID tag, when the reader and tag are separated by a medium consisting of brick and concrete materials. The second goal, is to measure the receive signal power strength at the location of the tag, where it is being successfully read by the reader. By using received power magnitude, we calculate the power loss between reader and tag. We compare the obtained values the theoretical results obtained by the channel power loss model given Chapter IV.

6.1 Experimental Setup

Impinj R420 [68] RFID Reader was used for the experimental study. Although the reader allows connecting four different antennas at the same time to provide wider reception angle, we used one antenna throughout the experiment. The antenna that was employed in the experiment is MT-243017/NRH [69]. The antenna is circularly polarized and has gain of $11dBic$, which is approximately equivalent to $9dBi$. Passive RFID Tag used in the experiment is Omni-ID Dura 3000 [41]. The tag has $35m$ read range with $30dBm$ transmit power in free space. The user memory of the tag is 512 bits. To operate the reader, Impinj MultiReader Software was used. By connecting the Impinj RFID Reader, the software can be used to send any C1Gen2 propocol command to tags. For spectrum analysis, we use Universal Software Radio Peripheral (USRP) [70] and GnuRadio [71] software. USRP is a software-defined radio that connects to a computer and serves as a wireless

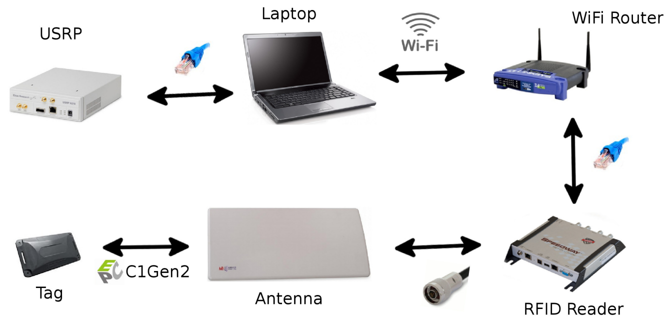

Figure 6.1: Experimental equipment diagram.

communication front-end. Gnuradio is a software toolkit to be usually used with an RF front-end hardware such as USRP. We used a software built on Gnuradio to display power magnitude of the signal present on USRP antenna.

The equipment diagram is shown in Fig. 6.1. The USRP is connected to a computer as mentioned earlier. The computer is connected through WiFi to the Router, that is also linked up with the RFID Reader. This provides an easy way to wirelessly control the reader from a computer.

6.2 Experimental Results

We carry out experiments and take measurements for three different media between tag and reader. In the first two cases, we take measurements and read the tag through brick wall and concrete slab mediums between the reader and the tag, respectively. The transmission power of the reader is set to $30dBm$ and hence with the effect of antenna gain, total EIPR is 39dBm.

In the first case, the medium is a $50cm$ wide brick wall. Reader antenna an USRP are placed on opposite sides of the wall to measure signal attenuation. Spectrum measurement obtained through USRP is given in Fig. 6.2(a). Received power, as it can be seen from the graph, is roughly $15dBm$, which corresponds to $24dB$ power loss. This value is compared to theoretical calculation using (4.1), which equals to $20.3dB$.

In the second case, measurements were taken for reinforced concrete medium. As a medium we use reinforced concrete floor separating two storeys of a Koç University building. The width of the reinforced concrete is $40cm$. Reader and antenna were placed on upper floor, with antenna facing down while tag and USRP were on the lower floor, with tag facing up. The measurement of received power is shown in Fig. 6.2(b). With $1m$ separation between antenna and USRP, receive power is $-10dBm$. Thus, measured power loss between antenna and tag is $-49dB$. Using power loss expression (4.1), the theoretical value of total power loss is $-46dBm$.

The third case was realized with a real rubble in an environment with ruins. Images of setup are given in Fig. 6.4. Fig. 6.4(a) shows the placement of antenna and tag with respect to rubble. Antenna is placed on top of the rubble as shown in Fig. 6.4(b) and tag, along with laptop and USRP, is put under the rubble as shown in Fig. 6.4(c). Fig. 6.4(d) shows other hardware.

Closer image of the medium between antenna and tag is given in Fig. 6.5. As it can be seen, the medium is made of both reinforced concrete and brick. Approximate width of concrete section is $40cm$ and width of brick section is $10cm$. During measurements, we fix the tag higher from the ground. The total distance between antenna and tag is around $1.2m$ at the time of measurements and reading. Fig. 6.3 shows receive power graph at the point of tag location. Measured power level by USRP is $-15dBm$, and therefore, power loss through the rubble can be characterized as $-54dBm$. The equivalent theoretical value for power loss is $-53dBm$, which is very close to experimentally measured power loss.

Slight discrepancies between the values in all cases are expected. Several parameters such as type of brick, type of concrete, gap between reinforced bars. Furthermore, it should also be noted that in the third case of the experiment, tag was only readable when directional antennas of tag and reader were face to face. This confirms that the fading on the channel is Rician.

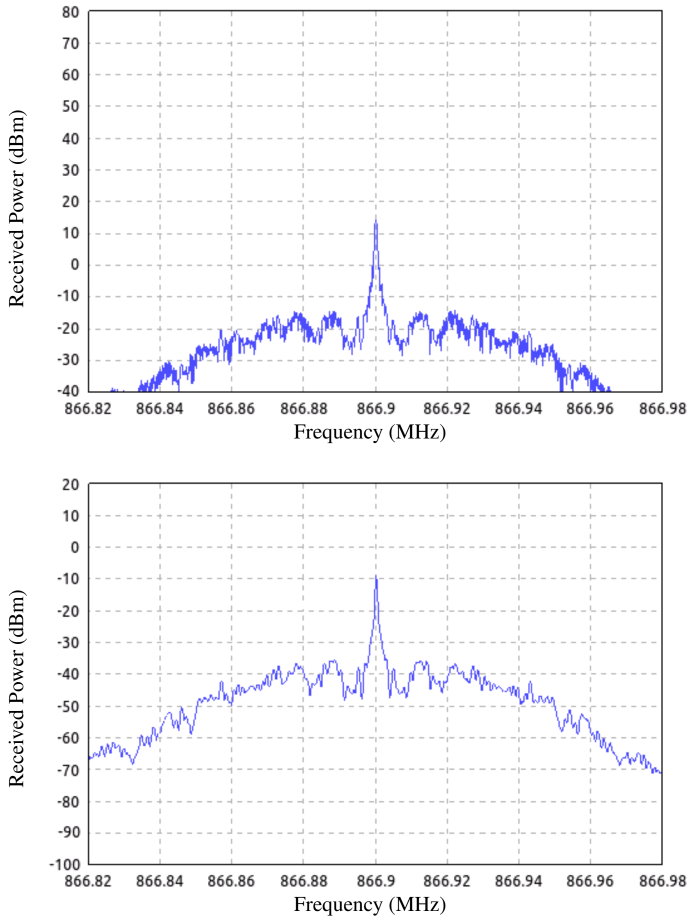

Figure 6.2: Measurements of receive power with mediums (a) brick and (b) concrete.

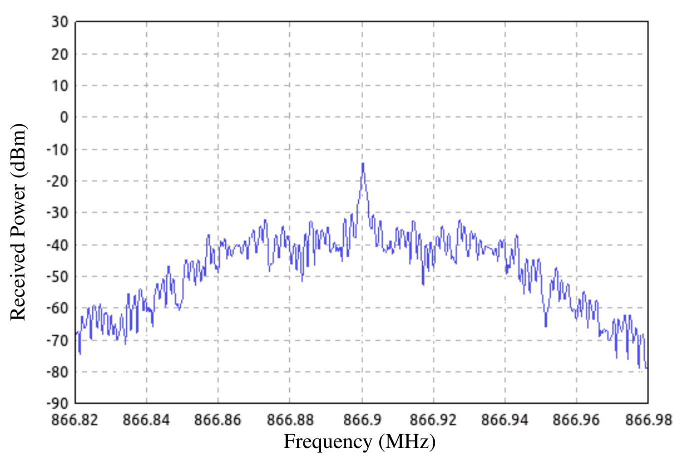

Figure 6.3: Measurements of receive power with in environment with ruins.

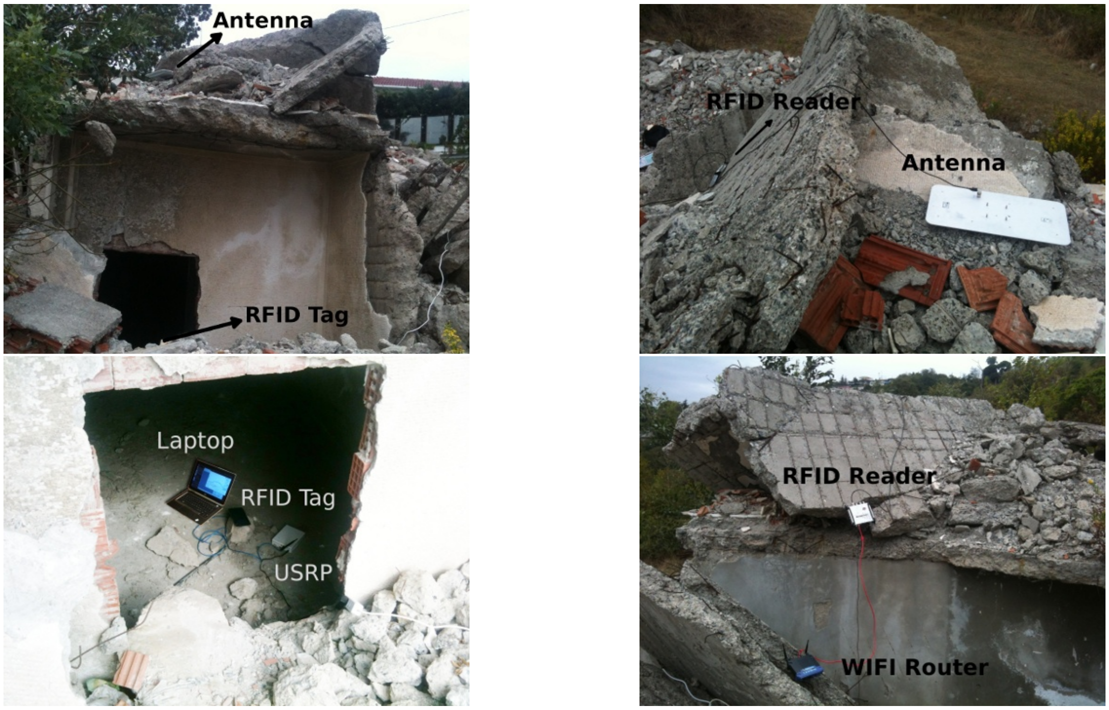

Figure 6.4: Images of experiment setup in the area with ruins.

Figure 6.5: Medium between antenna and passive RFID tag.

Chapter 7

CONCLUSION AND FUTURE RESEARCH DIRECTIONS

In this study, we evaluate the performance of passive communication through channel with collapsed building ruins. We propose RESCUE system that consists of a special RFID reader and sensors. Sensors store pictures of building interior taken at the time of an earthquake using sensor camera. After an earthquake, reader collects image data from sensors to estimate total number of victims left under ruins. Power loss equation is developed that takes into account multipath fading and shadowing effects. Moreover, we use an earthquake simulator to obtain different building ruins and these ruins are used in the theoretic study evaluate the performance of RESCUE. Total read time of all the sensors and corresponding transmission power values are calculated for various storey buildings. Finally, we present results of an experimental study. We successfully read a passive RFID tag in three different cases of medium type. We plot measured receive power levels and calculate the experimental power loss for all three cases. We plan to formulate more detailed channel model that takes into account additional effects such as diffraction, reflection and scattering. Future work for this study also include building the RESCUE system and testing it in collapsed building environments. We will carry out more rigorous experimental study where we will measure total operation time and required maximum transmission power.

REFERENCES

[1] "Israeli medical, rescue workers help haitians." http://www.jta.org/2010/01/17/news-opinion/world/israeli-medical-rescue-workers-help-haitians. Published: 2010-01-17.

[2] R. van der Togt, E. Beinat, S. Zlatanova, and H. J. Scholten, "Location interoperability services for medical emergency operations during disasters," in *Geo-information for disaster management*, pp. 1127–1141, Springer, 2005.

[3] "General and disaster rescue - australian emergency manual series." http://www.em.gov.au/Documents/Manual35-GeneralandDisasterRescue.pdf. Published: 2006, Manual Number: 35.

[4] "Technical handbook for search & rescue operations in earthquakes." http://ecpfe.oasp.gr/sites/default/files/Search&RescueOperationsinEarthequakes.pdf. EUROPEAN CENTRE ON PREVENTION AND FORECASTING OF EARTHQUAKES (ECPFE).

[5] Z. Xue and A. Chen, "Rescuability assessment model on casualties and application based on rfid," in *Cooperation and Promotion of Information Resources in Science and Technology, 2009. COINFO'09. Fourth International Conference on*, pp. 104–110, IEEE, 2009.

[6] Y.-C. J. Wu and C.-Y. Hung, "The use of rfid technology in earthquakes," *International Journal of Innovation and Sustainable Development*, vol. 4, no. 4, pp. 253–275, 2009.

[7] H. Yamada, S. Takaoka, and S. Hirose, "A snake-like robot for real-world inspection applications (the design and control of a practical active cord mechanism)," *Advanced Robotics*, vol. 27, no. 1, pp. 47–60, 2013.

[8] M. Donelli, "A rescue radar system for the detection of victims trapped under rubble based on the independent component analysis algorithm.," *Progress In Electromagnetics Research M*, vol. 19, 2011.

[9] M. Daito and N. Tanida, "Agent-based simulation approach for disaster rescue using active rfid," *The Review of Socionetwork Strategies*, vol. 1, no. 2, pp. 23–39, 2008.

[10] X. Ma, Q.-Y. Huang, and X.-M. Shu, "A new localization algorithm of mobile phone for outdoor emergency rescue," in *Intelligent System Design and Engineering Applications (ISDEA), 2013 Third International Conference on*, pp. 124–127, IEEE, 2013.

[11] O. B. Akan, M. T. Isik, and B. Baykal, "Wireless passive sensor networks," *Communications Magazine, IEEE*, vol. 47, no. 8, pp. 92–99, 2009.

[12] L.-S. Chai, J. He, and X.-C. Wei, "Radio channel modeling and measurement of a localization rescue system," in *Antennas & Propagation (ISAP), 2013 Proceedings of the International Symposium on*, vol. 2, pp. 1060–1063, IEEE, 2013.

[13] J. Wang, Z. Cheng, L. Jing, and T. Yoshida, "Design of a 3d localization method for searching survivors after an earthquake based on wsn," in *Awareness Science and Technology (iCAST), 2011 3rd International Conference on*, pp. 221–226, IEEE, 2011.

[14] L. Chen, M. Loschonsky, and L. M. Reindl, "Autoregressive modeling of mobile radio propagation channel in building ruins," *Microwave Theory and Techniques, IEEE Transactions on*, vol. 60, no. 5, pp. 1478–1489, 2012.

[15] N. Katahira, D. Isobe, T. Ine, and K. Kajiwara, "Development of macro-model seismic collapse simulator for framed structures using asi-gauss technique," *Proceedings of 14th WCEE (CD). Beijing: The 14th WVEE Organizing Committee*, 2008.

[16] M. Wille and F. Mattern, "Evaluation and optimization of rfid transmission control strategies," *Departament of Computer Science*, 2005.

[17] A. Shamdani and B. Nicolai, "Applications of rfid in incident management," in *ICCGI 2012,*

The Seventh International Multi-Conference on Computing in the Global Information Technology, pp. 34–39, 2012.

[18] H. Yang, L. Yang, and S.-H. Yang, "Hybrid zigbee rfid sensor network for humanitarian logistics centre management," *Journal of Network and Computer Applications*, vol. 34, no. 3, pp. 938–948, 2011.

[19] O. Takizawa, A. Shibayama, M. Hosokawa, K. Takanashi, M. Murakami, Y. Hisada, Y. Hada, K. Kawabata, I. Noda, and H. Asama, "Hybrid radio frequency identification system for use in disaster relief as positioning source and emergency message boards," in *Mobile Response*, pp. 85–94, Springer, 2007.

[20] H. Asama, Y. Hada, K. Kawabata, I. Noda, O. Takizawa, J.-i. Meguro, K. Ishikawa, T. Hashizume, T. Ohga, K. Takita, *et al.*, "Information infrastructure for rescue systems," in *Rescue Robotics*, pp. 57–69, Springer, 2009.

[21] A. Y. Chen, F. Peña-Mora, A. P. Plans, S. J. Mehta, and Z. Aziz, "Supporting urban search and rescue with digital assessments of structures and requests of response resources," *Advanced Engineering Informatics*, vol. 26, no. 4, pp. 833–845, 2012.

[22] O. Takizawa, "Rfid-based disaster-relief system," *Journal of the National Institute of Information and Communications Technology*, pp. 259–277, 2007.

[23] P. Bahl and V. N. Padmanabhan, "Radar: An in-building rf-based user location and tracking system," in *INFOCOM 2000. Nineteenth Annual Joint Conference of the IEEE Computer and Communications Societies. Proceedings. IEEE*, vol. 2, pp. 775–784, Ieee, 2000.

[24] L. Chen, M. Loschonsky, and L. M. Reindl, "Large-scale fading model for mobile communications in disaster and salvage scenarios," in *Wireless Communications and Signal Processing (WCSP), 2010 International Conference on*, pp. 1–5, IEEE, 2010.

[25] J. Walfisch and H. L. Bertoni, "A theoretical model of uhf propagation in urban environments," *Antennas and Propagation, IEEE Transactions on*, vol. 36, no. 12, pp. 1788–1796, 1988.

[26] H. Maruyama and K. Ito, "Semi-autonomous snake-like robot for search and rescue," in *Safety*

Security and Rescue Robotics (SSRR), 2010 IEEE International Workshop on, pp. 1–6, IEEE, 2010.

[27] M. Loschonsky, C. Feige, O. Rogall, S. Fisun, and L. Reindl, "Detection technology for trapped and buried people," in *Wireless Sensing, Local Positioning, and RFID, 2009. IMWS 2009. IEEE MTT-S International Microwave Workshop on*, pp. 1–6, IEEE, 2009.

[28] A. Yarovoy, L. Ligthart, J. Matuzas, and B. Levitas, "Uwb radar for human being detection," *Aerospace and Electronic Systems Magazine, IEEE*, vol. 21, no. 3, pp. 10–14, 2006.

[29] S. Z. Gürbüz, W. L. Melvin, and D. B. Williams, "Detection and identification of human targets in radar data," in *Defense and Security Symposium*, pp. 65670I–65670I, International Society for Optics and Photonics, 2007.

[30] M. Bimpas, K. Nikellis, N. Paraskevopoulos, D. Economou, and N. Uzunoglu, "Development and testing of a detector system for trapped humans in building ruins," in *Microwave Conference, 2003. 33rd European*, vol. 3, pp. 999–1002, IEEE, 2003.

[31] S. Zorn, M. Maser, A. Goetz, R. Rose, and R. Weigel, "A power saving jamming system for e-gsm900 and dcs1800 cellular phone networks for search and rescue applications," in *Wireless Sensors and Sensor Networks (WiSNet), 2011 IEEE Topical Conference on*, pp. 33–36, IEEE, 2011.

[32] A. Goetz, S. Zorn, R. Rose, G. Fischer, and R. Weigel, "A time difference of arrival system architecture for gsm mobile phone localization in search and rescue scenarios," in *Positioning Navigation and Communication (WPNC), 2011 8th Workshop on*, pp. 24–27, IEEE, 2011.

[33] C. Feige, T. Ostertag, M. Loschonsky, and L. M. Reindl, "Radar assisted detection of passive electronic components," in *Radio and Wireless Symposium (RWS), 2010 IEEE*, pp. 200–203, IEEE, 2010.

[34] S. Zorn, R. Rose, A. Goetz, and R. Weigel, "A novel technique for mobile phone localization for search and rescue applications," in *Indoor Positioning and Indoor Navigation (IPIN), 2010 International Conference on*, pp. 1–4, IEEE, 2010.

[35] E. EPCglobal, “Radio-frequency identity protocols class-1 generation-2 uhf rfid protocol for communications at 860 mhz–960 mhz version 1.0. 9,” *K. Chiew et al./On False Authenticationsfor C1G2 Passive RFID Tags*, vol. 65, 2004.

[36] “Earthquakes with 1,000 or more deaths since 1900.” `http://earthquake.usgs.gov/earthquakes/world/world_deaths.php`.

[37] P. Semiconductors, “The i2c-bus specification,” *Philips Semiconductors*, vol. 9397, no. 750, p. 00954, 2000.

[38] S. Kuhr, *Implementation of a JPEG Decoder for a 16-bit Microcontroller*. PhD thesis, UNIVERSITY OF APPLIED SCIENCES, 2002.

[39] “Top 10 reasons for using ultracapacitors in your system designs.” `http://www.maxwell.com/products/ultracapacitors/docs/top_10_reasons_for_ultracaps.pdf`.

[40] R. Signorelli, J. Schindall, and J. Kassakian, “Carbon nanotube enhanced ultracapacitor,” 2006.

[41] “Omni-id dura 3000.” `http://www.omni-id.com/pdfs/Omni-IDDura3000datasheet.pdf`.

[42] J. Kyynäräinen, J. Saarilahti, H. Kattelus, A. Kärkkäinen, T. Meinander, A. Oja, P. Pekko, H. Seppä, M. Suhonen, H. Kuisma, *et al.*, “A 3d micromechanical compass,” *Sensors and Actuators A: Physical*, vol. 142, no. 2, pp. 561–568, 2008.

[43] A. Raychowdhury and K. Roy, “Carbon nanotube electronics: design of high-performance and low-power digital circuits,” *Circuits and Systems I: Regular Papers, IEEE Transactions on*, vol. 54, no. 11, pp. 2391–2401, 2007.

[44] Texas Instruments, “Low dropout regulator for 5v to 3.3v conversion.” LM3940 datasheet.

[45] W. Lu and L. Dai, “Carbon nanotube supercapacitors,” 2010.

[46] Texas Instruments, “16-bit mixed signal microcontroller.” MSP430F5328EP datasheet.

[47] Measurement Specialities, "Triaxial piezoelectric accelerometer." 832-0200 datasheet.

[48] Toshiba, "Cmos vga camera module." TCM8230MD (A) datasheet.

[49] "Tego pioneering new generation rfid." `http://tegoinc.com/tego-products/chips/`.

[50] Vina Tech, "5v 7.5f ultracapacitor." VEC5R0755QG datasheet.

[51] Vina Tech, "3v 500f ultracapacitor." VEC3R0507QA datasheet.

[52] MAXIM, "220vac to 5.0vdc ac-to-dc regulator." MAX160 datasheet.

[53] Analog Devices, "Cmos low power dual 2:1 mux/demux switch." ADG787 datasheet.

[54] F. C. Schoute, "Dynamic frame length aloha," *Communications, IEEE Transactions on*, vol. 31, no. 4, pp. 565–568, 1983.

[55] A. F. Molisch, *Wireless communications*, vol. 15. John Wiley & Sons, 2010.

[56] C. A. Balanis, *Advanced engineering electromagnetics*, vol. 205. Wiley New York, 1989.

[57] D. Pena, R. Feick, H. D. Hristov, and W. Grote, "Measurement and modeling of propagation losses in brick and concrete walls for the 900-mhz band," *Antennas and Propagation, IEEE Transactions on*, vol. 51, no. 1, pp. 31–39, 2003.

[58] S. Y. Seidel and T. S. Rappaport, "914 mhz path loss prediction models for indoor wireless communications in multifloored buildings," *Antennas and Propagation, IEEE Transactions on*, vol. 40, no. 2, pp. 207–217, 1992.

[59] L. Chen, T. Ostertag, M. Loschonsky, and L. M. Reindl, "Measurement of mobile radio propagation channel in ruins," in *Wireless Communications, Networking and Information Security (WCNIS), 2010 IEEE International Conference on*, pp. 252–256, IEEE, 2010.

[60] A. Goldsmith, *Wireless communications*. Cambridge university press, 2005.

[61] M. Simon and D. Divsalar, "Some interesting observations for certain line codes with application to rfid," *IEEE transactions on communications*, vol. 54, no. 4, pp. 583–586, 2006.

[62] J. Sanchez-Garcia and D. R. Smith, "Capture probability in rician fading channels with power control in the transmitters," *IEEE transactions on communications*, vol. 50, no. 12, pp. 1889–1891, 2002.

[63] G. H. Golub and J. H. Welsch, "Calculation of gauss quadrature rules," *Mathematics of Computation*, vol. 23, no. 106, pp. 221–230, 1969.

[64] C. W. Cryer, "Rodrigues'formula and the classical orthogonal polynomials.," tech. rep., DTIC Document, 1968.

[65] J. Smith, *Modern communication circuits*. McGraw-Hill, Inc., 1986.

[66] J. Cousins, "Estimated damage and casualties from earthquakes affecting auckland city: a report prepared for the auckland city council," *Institute of Geological & Nuclear Sciences (GNS), Lower Hutt, New Zealand*, 2005.

[67] "Fx9500 fixed rfid reader." `http://www.motorolasolutions.com/web/Business/Products/RFID/RFIDReaders/FX9500/_Documents/FX9500_Specifications.pdf`.

[68] I. Speedway, "R420 rfid reader."

[69] "Specification for mt-243017/nrh rhcp reader antenna 865-870 mhz, 11 dbic." `http://www.mtiwe.com/Uploads/dbsAttachedFiles/MT-243017-NRHEngSpec.pdf`.

[70] M. Ettus, "Universal software radio peripheral (usrp)," *Ettus Research LLC* *`http://www.ettus.com`*, 2008.

[71] E. Blossom, "Gnu radio: tools for exploring the radio frequency spectrum," *Linux journal*, vol. 2004, no. 122, p. 4, 2004.

CURRICULUM VITAE

Orkhan Badirkhanli has received his B.S. degree in Electrical and Electronics Engineering from Middle East Technical University, Ankara, Turkey. He received his M.S. degree under supervision of Prof.Dr. Ozgur Baris Akan in Electrical and Electronics Engineering from Koc University, Istanbul, Turkey. His research interests include passive communication and wireless sensor networks.